Electronic Supplementary Material (ESI) for Journal of Materials Chemistry B.

Decellularized Matrix Enriched Collagen Microscaffold for a 3D Liver *In-Vitro* Model

[#]Shreemoyee De[a], [#]Ashwini Vasudevan[b], Dinesh M Tripathi[b] [*]Savneet Kaur[b] and [*]Neetu Singh [a,c]

a Centre for Biomedical Engineering, Indian Institute of Technology Delhi, Hauz Khas, New Delhi-110016, India

b Department of Molecular and Cellular Medicine, Institute of Liver and Biliary Sciences, D1, Vasant Kunj Marg, New Delhi, Delhi 110070

c Biomedical Engineering Unit, All India Institute of Medical Sciences, Ansari Nagar, New Delhi-110029, India

Email: shreemoyee.de@iitd.ac.in[a], ashwinivasudevan@yahoo.com[b], dineshmanitripathi@gmail.com[b], savykaur@gmail.com[b], sneetu@iitd.ac.in[a,c].

[#]have contributed equally

Corresponding Author

Dr. Savneet Kaur

Associate Professor,

Department of Molecular and Cellular Medicine,

Institute of Liver and Biliary Sciences, D1,

Vasant Kunj Marg, New Delhi-110070

Email- savykaur@gmail.com

Dr. Neetu Singh

Associate Professor, Centre for Biomedical Engineering,

Indian Institute of Technology Delhi, Hauz Khas, New Delhi-110016

Ph. No.- 011-26591422

Email- sneetu@iitd.ac.in

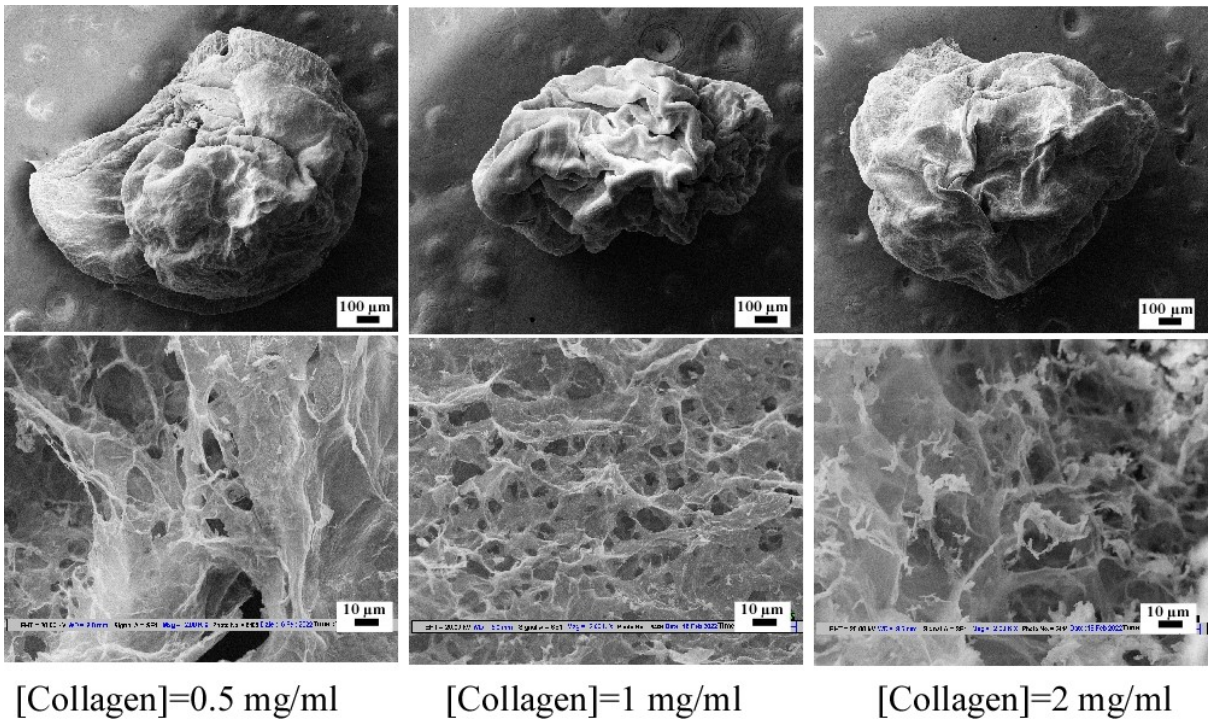

Figure S1: SEM micrographs for the microscaffolds with varying concentration of collagen. Changing the collagen concentrations effects the porosity of the microscaffold.

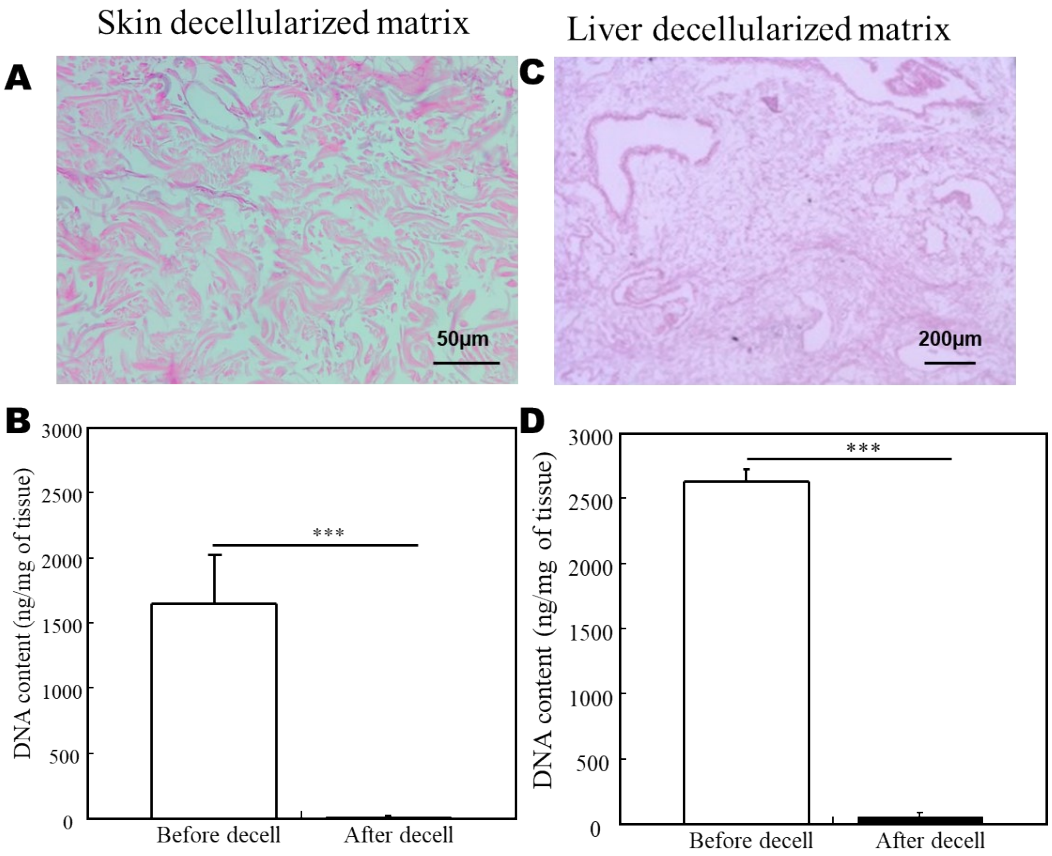

Figure S2: A. H&E staining of decellularized skin scaffold. B. DNA content of the native skin versus the decellularized skin scaffolds (***P < 0.001). C. H&E staining of decellularized liver scaffold. D. DNA content of the native liver versus the decellularized liver scaffolds (***P < 0.001).

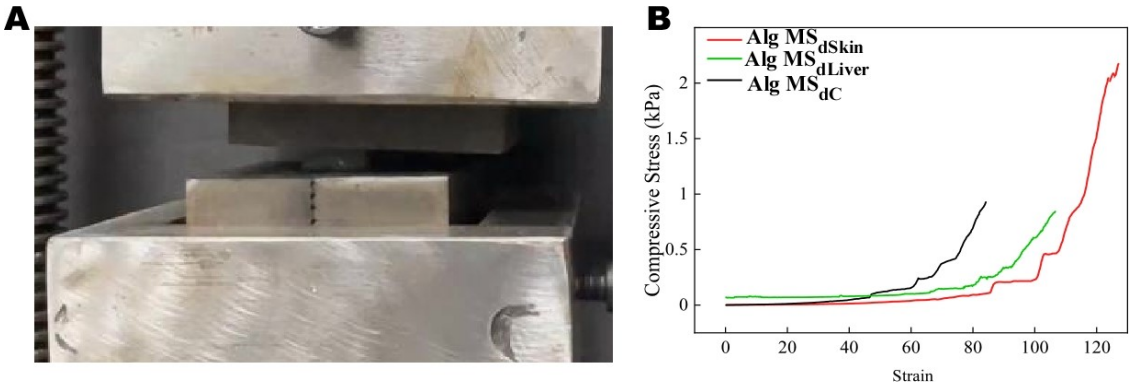

Figure S3: **A.** Image of the instrument used for compressive test. **B.** Graph showing mechanical properties of scaffolds (stress *vs* strain plots) under compressive loading.

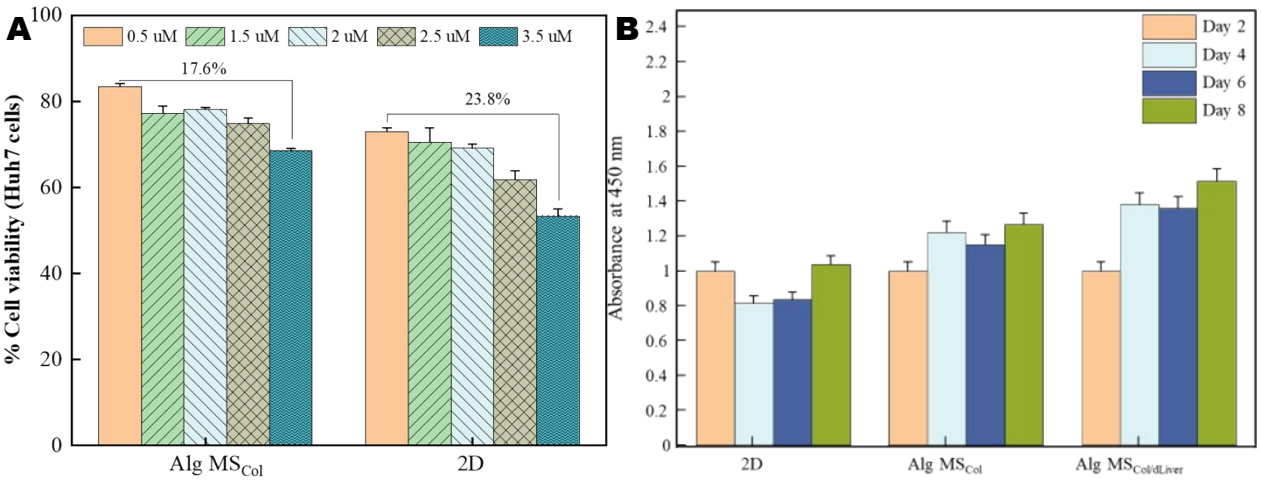

Figure S4: A. Alamar blue assay for Huh7 cells grown in 3D micro-scaffolds (Alg MS_{Col}) and on tissue culture plates (2D). The graph shows that after treatment with doxorubicin the viability in tissue culture plate is the lowest. In comparison, the same concentration results in lesser decrease in cell viability for cells encapsulated in micro-scaffolds. This clearly demonstrates the fact that slightly higher drug concentration is required to achieve effective cell death in 3D conditions and a concentration achieved by 2D culture may not result in similar effects. The graph plot is an average of two biological replicate and three technical replicates

for each sample. **B.** Albumin protein expression in the supernatant estimated by ELISA of the HuH7 cells grown in 2D and encapsulated in microscaffolds (Alg MS_{Col} and Alg $MS_{Col/dLiver}$). The graph plot is an average of two biological replicates and two technical replicates each.

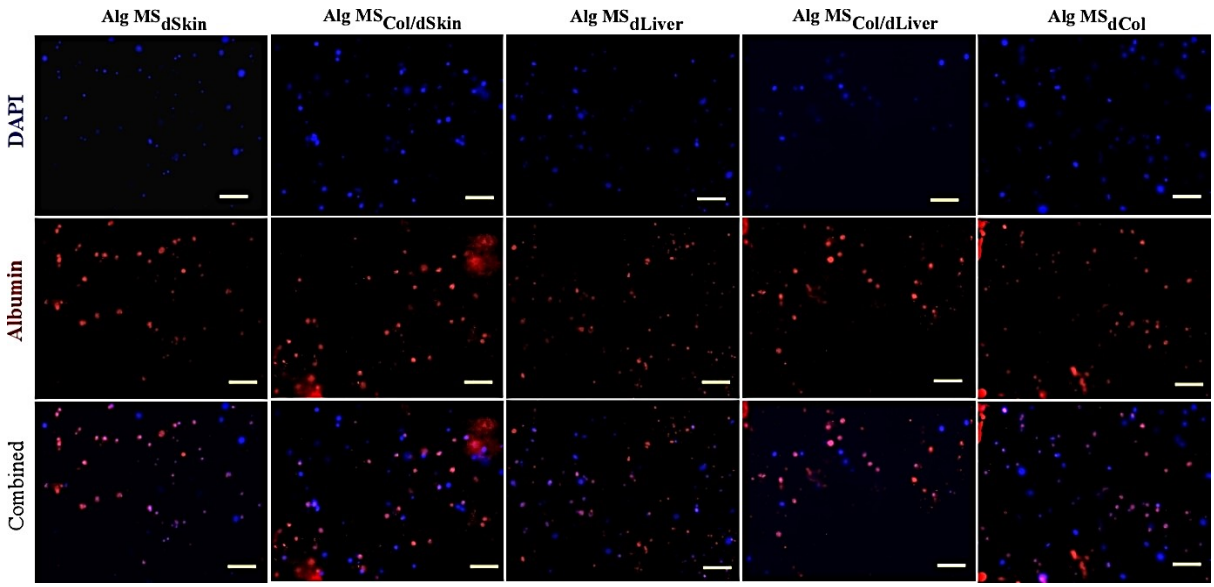

Figure S5: Immunofluorescence images of albumin expression in primary hepatocytes encapsulated in different microscaffolds taken on day 2 after encapsulation (Blue: DAPI; Red: Albumin staining) observed under 10x objective. (Scale bar: 200 µm)

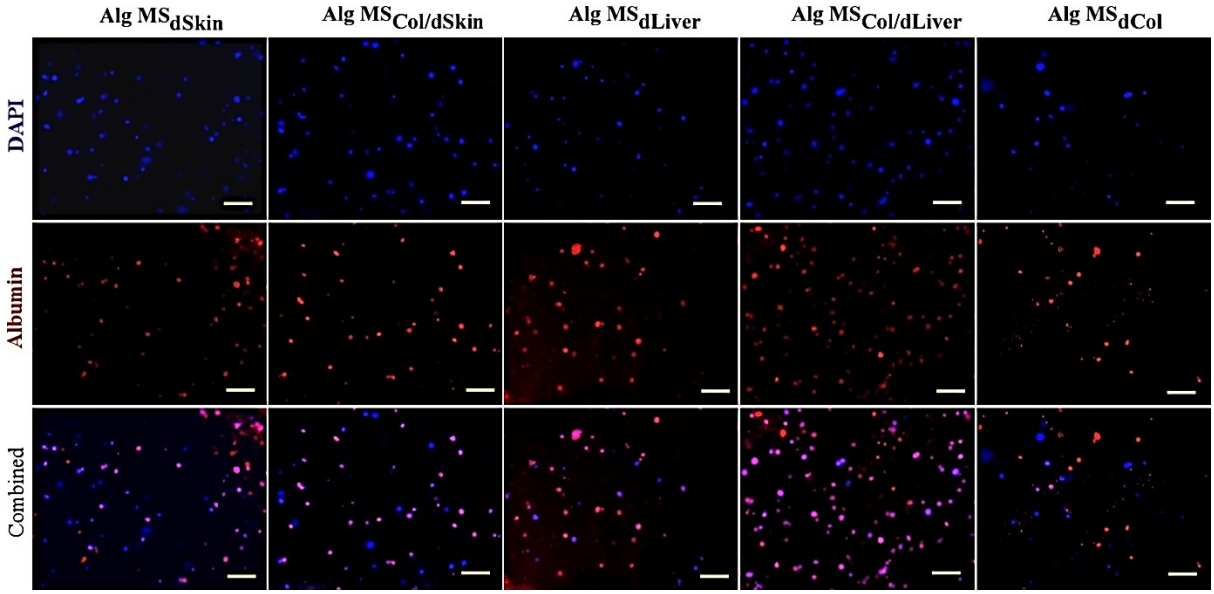

Figure S6: Immunofluorescence images of albumin expression in primary hepatocytes encapsulated in different microscaffolds taken on day 14 after encapsulation (Blue: DAPI; Red: Albumin staining) observed under 10x objective. (Scale bar: 200 µm).

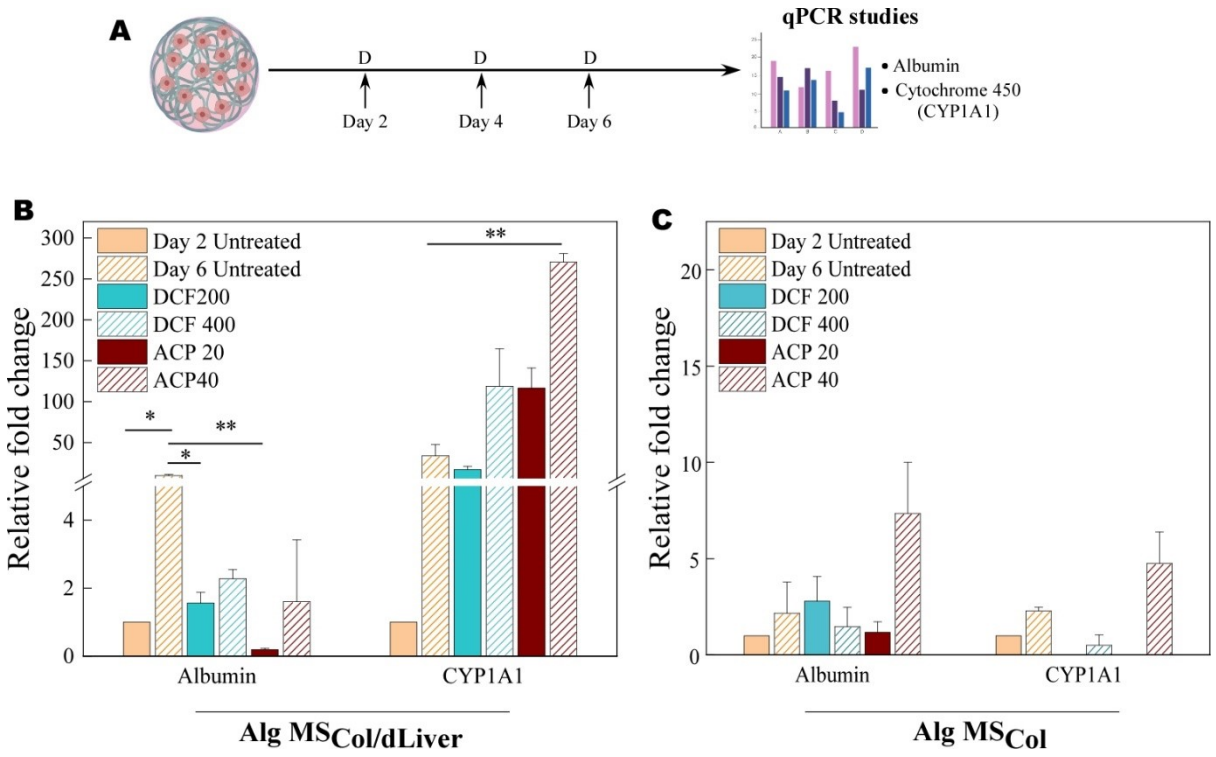

Figure S7: **A**. Experiment schematic for studying drug toxicity in the microscaffold platform developed. **B.** Albumin and CYP1A1 expression as analyzed by qPCR in the extracted hepatocytes after 6 days of drug treatment while encapsulated in the microscaffold containing collagen with liver dECM. **C**. Albumin and CYP1A1 expression as analyzed by qPCR in the extracted hepatocytes after 6 days of drug treatment while encapsulated in the microscaffold containing only collagen.